DETECTION OF 25-YEAR LAND-COVER CHANGE IN A CRITICAL WATERSHED IN SOUTHERN PHILIPPINES USING LANDSAT MSS AND ETM+ IMAGES: IMPORTANCE IN WATERSHED REHABILITATION

J. R. Santillan [a, *], M. M. Makinano [b], E. C. Paringit [a]

[a] Research Laboratory for Applied Geodesy and Space Technology, Department of Geodetic Engineering, University of the Philippines (UP), Diliman, Quezon City 1101, Philippines – jrsantillan@up.edu.ph, ecp@engg.upd.edu.ph
[b] College of Engineering and Information Technology, Caraga State University (CSU), Ampayon, Butuan City 8600, Philippines – meriam.makinano@gmail.com

KEY WORDS: Land Cover, Hydrology, Impact Analysis, Modelling, Landsat

ABSTRACT:

We analyzed Landsat MSS and ETM+ images to detect 25-year land-cover change (1976-2001) in the critical Taguibo Watershed in Mindanao Island, Southern Philippines. This watershed has experienced historical modifications of its land-cover due to the presence of logging industries in the 1960s, and continuous deforestation due to illegal logging and slash-and-burn agriculture in the present time. To estimate the impacts of land-cover change on watershed runoff, we utilized the land-cover information derived from the Landsat images to parameterize a GIS-based hydrologic model. The model was then calibrated with field-measured discharge data and used to simulate the responses of the watershed in its year 2001 and year 1976 land-cover conditions. The availability of land-cover information on the most recent state of the watershed from the Landsat ETM+ image made it possible to locate areas for rehabilitation such as barren and logged-over areas. We then created a "rehabilitated" land-cover condition map of the watershed (re-forestation of logged-over areas and agro-forestation of barren areas) and used it to parameterize the model and predict the runoff responses of the watershed. Model results showed that changes in land-cover from 1976 to 2001 were directly related to the significant increase in surface runoff. Runoff predictions showed that a full rehabilitation of the watershed especially in barren and logged-over areas will likely to reduce the generation of huge volume of runoff during rainfall events. The results of this study have demonstrated the usefulness of multi-temporal Landsat images in detecting land-cover change, in identifying areas for rehabilitation, and in evaluating rehabilitation strategies for management of tropical watersheds through its use in hydrologic modeling.

1. INTRODUCTION

Human-induced land-cover changes pose negative impacts to watershed ecosystems. It has been widely recognized that changes such as forest cover reduction through deforestation and conversion for agricultural purposes can alter a watershed's response to rainfall events, that often leads to increased volumes of surface runoff and greatly increase the incidence of flooding (McColl and Aggett, 2007; Cebecauer and Hofierka, 2008). The detection of these changes is crucial to provide information as to what and where the changes have occurred and to analyze these changes in order to formulate proper mitigation measures and rehabilitation strategies.

Remote sensing (RS) techniques have been used extensively to provide accurate and timely information describing the nature and extent of land resources and changes over time. In watershed research and hydrological sciences, RS has played a major role because of its ability to provide spatially continuous data, its potential to provide measurements of hydrological variables not available through traditional techniques, and its ability to provide long term, global-wide data, even for remote and generally inaccessible regions of the Earth (Engman, 1996). It is perhaps for land-cover data derivation that RS has made its largest impact and comes closest to maximize its capabilities in watershed research (Engman, 1995). This has prompted researchers and watershed planners to exploit land-cover information derived from remotely-sensed images in a variety of hydrological modeling studies, most especially in surface runoff predictions (Melesse and Shih, 2002; Bach et al., 2003; Pandey et al., 2008). The addition of Geographic Information System (GIS) technology further enhanced these capabilities and added confidence in the accuracy of modeled watershed conditions, improved the efficiency of the modeling process and increased the estimation capability of hydrologic models (Bhuyan, et al., 2003).

A common approach in integrated RS-GIS-Modeling for event-based watershed runoff predictions usually involves (1) the derivation of land-cover related parameters of the models from remotely-sensed images, (2) the use of GIS to prepare the model and to extract additional parameters, (3) calibration and validation of the model using field measured data to test its efficiency, and then (4) use the model to simulate runoff and use the simulated information to characterize the conditions of the watershed (O'Connell, et al., 2007; Vafeidis, et al., 2007). For land-cover change impact predictions in watersheds, the same approach is generally followed except that the model is run first for an initial land-cover condition, then the land-cover related parameters of the models are altered to reflect the change, and the model is re-run (O'Connell, et al., 2007). The effect of the change is estimated based on the differences between the runoff hydrographs simulated in the initial and "changed" conditions, respectively. Several studies have utilized the RS-GIS-Modeling approach for assessing the impacts of land-cover change to the hydrologic response of

* Corresponding author.

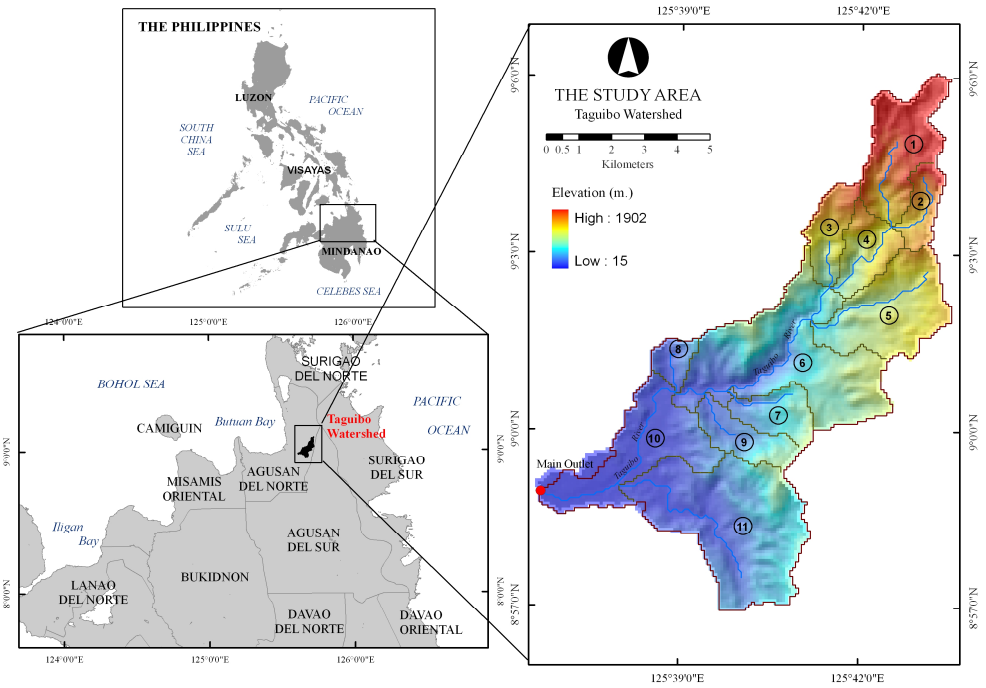

Figure 1. The Taguibo Watershed in Mindanao Island, Philippines

watersheds to rainfall events (e.g., Helmschrot and Flügel, 2002; McColl and Aggett, 2007; Leblanc, et al., 2008). However, a majority of them is focused on modeling the hydrological response of watersheds to future changes in land-cover. Very few studies relate the hydrological responses of watershed to its past and present conditions. In watershed management, this is of paramount importance as the information derived from modeling can be directly related to the changes in land-cover as well as to the overall condition of the modelled watershed. Proper mitigation measures and efficient conservation strategies can then be formulated upon examination of the root causes of watershed problems, and hence, leading to its rehabilitation.

The location and nature of change which has occurred in a watershed can be explicitly recognized using a post-classification comparison approach of land-cover change detection from RS images (Coppin et al., 2004). This approach uses separate classifications of images acquired at different times to produce difference maps from which ‘‘from–to’’ change information can be generated (Jensen, 2004). Among the several classifiers available, the Maximum Likelihood Classifier (MLC) has been widely used to classify RS data and successful results of applying this classifier for land-cover mapping have been numerous (e.g., Cherrill et al., 1994; Cingolani, et al., 2004; Hagner and Reese, 2007) despite its limitations due to its assumption of normal distribution of class signatures (Swain and Davis, 1978). Its use has also been effective in a number of post-classification comparison change detection studies (e.g., Helmschrot and Flügel 2002; Muttitanon and Tripathi 2005; Chowdhury 2006; Vagen 2006). While recent studies have indicated the superiority over MLC of newly developed image classifications techniques based on decision trees (DT), neural networks (NN) and support vector machines (SVM) (e.g., Huang et al., 2002; Shuying et al., 2005; Otukei and Blaschke 2010), the advantage of MLC over these classifiers remains to be significant owing to its simplicity and lesser computing time. This is very crucial, especially for rapid land-cover mapping and change detection analysis of numerous multi-temporal images. Moreover, the accuracy of any classifier is affected by the number of training samples and by selecting which bands to use during the classification. As reported by Huang et al. (2002), improved classification accuracies of MLC, DT, NN and SVM can be achieved when training data size is increased and when more bands are included. In the case of Landsat image classification, improvements due to the inclusion of all bands exceeded those due to the use of a better classifier or increased training data size, underlining the need to use as much information as possible in deriving land cover classification from RS images (Huang et al., 2002).

In these contexts, our goal here is to exemplify the importance of land-cover change detection by RS image analysis to provide relevant information on past and present conditions of a watershed. Specifically, we applied post-classification comparison analysis of Maximum Likelihood-classified Landsat MSS and ETM+ images to detect 25-year land-cover change in the critical Taguibo Watershed in Mindanao Island, Southern Philippines. We then relate the changes in land-cover to the responses of the watershed to rainfall events using a GIS-based hydrologic model. The model is also used to test planned rehabilitation measures and strategies to approximate their success or failure in addressing the problems of the Taguibo Watershed

2. THE STUDY AREA

The Taguibo Watershed in the province of Agusan del Norte in the island of Mindanao, Philippines (Figure 1) is a region that has experienced extensive alteration of its land-cover ever since the start of operation of several logging industries with Timber License Agreements (TLAs) in the 1960’s until the early 1980s (DENR, 2003). Its forest cover was severely reduced by logging and clear-felling, and the former logged-over areas were opened up to intensive farming, thereby accommodating the influx of farmers who were intent in cultivating semi-temperature high value vegetables. More than 25 years later, a recent report by the Department of Environment and Natural Resources (DENR,

2003) indicated a very serious condition of the watershed: significant increase in runoff volume during rainfall events and extensive sedimentation of rivers and streams due to proliferations of eroded areas in the watershed's landscape. While it has yet to be proven, the DENR asserted that the denudation of the watershed's forest cover and its conversion to grasslands as well as for agricultural purposes are the prime reasons for the occurrence of these problems. The situation was further aggravated by the continuous presence of illegal logging and slash-and-burn farming activities in the upland portions of the watershed (DENR, 2003). These alarming situations have prompted the DENR to come up with rehabilitation efforts such as reforestation of formerly logged areas and agro-forestation in highly eroded landscapes to mitigate the problem of increased runoff generation and high rate of sedimentation. While these efforts to address the negative impacts of land-cover change on hydrological functions are necessary, they can only be fruitful if information on the location and extent of the areas that need rehabilitation is available. Moreover, relevant information that portrays space-time relationships of land-cover to hydrological functions is often required to formulate proper mitigation measures and efficient conservation strategies. All of these can be achieved through analysis of multitemporal RS images and hydrologic modeling.

The Taguibo Watershed has a drainage area of 75.532 km^2. It is composed of plains, steep hills and mountains. According to the Taguibo River Watershed Management Plan (DENR, 2003), majority of the soils in the watershed belongs to hydrologic soil group B (loamy and silty-loamy soils) which indicates medium runoff potential (SCS, 1985). Clayey and shallow soils belonging to hydrologic soil group D (high runoff potential) are generally observed in areas with 50% or more slope. The study area has no distinct dry season; pronounced rainfall occurs from November to January.

3. METHODS

3.1 Landsat image analysis and change detection

Orthorectified Landsat MSS and ETM+ images covering the study area acquired on April 17, 1976 (path 120, row 54) and May 22, 2001 (path 112, row 54), with pixel resolution of 57-m and 28.5-m, respectively, were obtained from the Global Land-cover Facility (GLCF), University of Maryland (http://glcf.umiacs.umd.edu). These images are part of the GLCF GeoCover collection which consists of decadal Landsat data which has been orthorectified and processed to a higher quality standard. Documentations on the orthorectification process can be found in the GLCF GeoCover website at http://glcf.umiacs.umd.edu/research/portal/geocover/.

The images were radiometrically corrected to at-sensor radiance using the standard Landsat calibration formulas and constants. A fast atmospheric correction using dark-object subtraction (Schowengerdt, 1997) was also implemented. Normalised Difference Vegetation Index (NDVI) images were also computed from the radiometrically and atmospherically-corrected images. Only the portions of the images covering the study area were subjected to image analysis. Six (6) land-cover classes were identified from the images through visual interpretations with the aid of existing land-cover and topographic maps published by the DENR as references. These include barren areas, built-up areas, forest, grassland, mixed vegetation (combination of forest, tree plantation, shrub land and grassland) and water bodies. In this study, barren areas are defined as those portions of the watershed with exposed soil and in which less than half of an areal unit has vegetation or other cover while built-up areas are those portions of intensive human use with much of the land covered by structures. The forest class is defined as parcels of land having a tree-crown areal density of 10% or more and are stacked with trees capable of producing timber or other wood products. Grasslands are those portions where the natural vegetation is predominantly grasses and/or grass-like plants.

Built-up areas were only detected on the 2001 Landsat ETM+ image. We assumed that built-up areas in the 1976, although present, were limited in extent so that they were not visible in the Landsat MSS images primarily because of the sensor's low spatial resolution. Representative samples of each class were collected from the images for supervised image classification. The training samples were collected in such a way that the assumption of normal distribution of the MLC is satisfied and that the separability of the classes (computed using the Jeffries-Matusita Distance) (Richards and Jia, 1997) is ≥ 1.7. Another independent set of samples were likewise collected for accuracy assessment. A minimum number of 30 ground truth pixels were randomly chosen for each class, following the guidelines of Van Genderen et al. (1978) to obtain a reliable estimate of classification accuracy of at least 90%.

The MLC was used to classify the Landsat images with the inclusion of the NDVI. The accuracy of each classified images were independently assessed. Four measures were used to assess the accuracy of the classified images namely, the overall classification accuracy, kappa statistic, producer's accuracy (PA) and user's accuracy (UA). Initial trials were done to classify the input images using the Minimum Distance, Mahalanobis Distance and Parallepiped classifiers. However, the accuracies of each classified image using these classifiers were significantly lower (<90%) than those of the MLC-classified images. The two resulting land-cover maps were then subjected to post-classification comparison change detection analysis to examine the location, extent and distribution of land-cover change in the study area. The 2001 land-cover map was first re-sampled to 57-m resolution prior to change detection.

3.2 Hydrologic modelling

Hydrologic modeling was performed using the Soil Conservation Service-Curve Number (SCS-CN) model (SCS, 1985). The SCS-CN model, also called the runoff curve number method, for the estimation of direct runoff from storm rainfall is a well established method in hydrologic engineering and environmental impact analyses and has been very popular because of its convenience, simplicity, authoritative origins, and its responsiveness to four readily grasped watershed properties: soil type, land-use/land-cover and treatment, surface condition, and antecedent moisture condition (Ponce and Hawkins, 1996). The popular form of the SCS-CN model is:

$$Q = \frac{(P - I_a)^2}{P - I_a + S} \quad for\ I_a \leq P,\ otherwise\ Q = 0 \tag{1}$$

$$I_a = \lambda S \tag{2}$$

$$S = \frac{25400}{CN} - 254 \tag{3}$$

where P is total rainfall, I_a is initial abstraction, Q is direct runoff, S is potential maximum retention which can range (0, ∞), and λ is initial abstraction coefficient or ratio. All variables are in millimeters (mm) except for λ which is unitless. The initial abstraction I_a includes short-term losses due to evaporation, interception, surface detention, and infiltration and its ratio to S describes λ which depends on climatic conditions and can range (0, ∞). The SCS has adopted a standard value of 0.2 for the initial abstraction ratio (SCS, 1985) but this can be estimated through calibration with field measured hydrologic data. The potential maximum retention S characterizes the watershed's potential for abstracting and retaining storm moisture, and therefore, its direct runoff potential (Ponce and Hawkins, 1996). S is directly related to land-cover and soil infiltration through the parameter *CN* or "curve number", a non-dimensional quantity varying in the range (0–100) and depends on the antecedent moisture condition of the watershed. Higher *CN* values indicate high runoff potential. For normal antecedent moisture conditions (AMCII, 5-day antecedent rainfall (AR) is 0.5 – 1.1 inches), the curve number values for land-cover types and soil textures (hydrologic soil groups B and D) prevalent in the study area are shown in Table 2. The AMCII CN values can be converted to AMCI (dry condition, AR<0.5 inches) and AMCIII (wet condition, AR>1.1 inches) using the formula of Chow, et al. (1988).

Land-cover	AMCII Curve Number (*CN*)	
	Soil Group B	Soil Group D
Barren areas	86	94
Built-up areas	74	86
Forest	55	77
Grassland	61	80
Mixed Vegetation	58	79
Water	98	98

Table 2. AMCII CN values for different land-cover types under hydrologic soil groups B and D which are prevalent in the study area. (Source: SCS, 1985)

The SCS-CN model was implemented using the Hydrologic Engineering Center-Hydrological Modeling System or HEC-HMS (USACE, 2000). The SCS-CN model was co-implemented with the Clark Unit Hydrograph method (for sub-watershed routing of runoff), the Exponential Baseflow Recession model, and the Muskingum-Cunge model for channel routing. A thorough discussion of these three additional models can be found in Chow et al. (1988). Model parameterizations were done using HEC-GeoHMS (USACE, 2003), the ArcView GIS-based pre-processor of HEC-HMS. HEC-GeoHMS was used to delineate 11 sub-watershed boundaries and reproduce topologically-correct stream network through a series of steps collectively known as terrain pre-processing, by utilizing the surface topography information from a Shuttle Radar Topography Mission (SRTM) DEM as the origin of the boundaries and stream network. Average *CN* values for each sub-watershed were computed based on the 2001 and 1976 land-cover maps. Sub-watershed time of concentration and storage coefficient parameters of the Clark Unit Hydrograph model as well as initial values of the recession constant in each sub-watershed were first assumed but these values were later optimized during the calibration stage. Muskingum-Cunge model parameter values were obtained from river profile and cross-section surveys.

The HEC-HMS model was calibrated using rainfall events recorded at the inner portion of the watershed, and discharge hydrographs measured at the main outlet for the June 25-27, 2007 period. Records of 5-day accumulated rainfall depths before the simulation showed an AR>1.1 inches, indicating AMCIII. Hence, the AMCII values were transformed to AMCIII using Chow, et al. (1988)'s formula. Model calibration was done to fine-tune the λ parameter of the SCS-CN model, and the time-related parameters of the Exponential Baseflow Recession model and Clark Unit Hydrograph model, which were initially assumed. The absence of sources of land-cover information for the state of the watershed when the calibration data were collected prompted us to parameterize the model using the 2001 land-cover map. During this period, available satellite images were all covered with clouds. We assumed that no significant change in land-cover had occurred from 2001-2007. The Nash-Sutcliffe (1970) Coefficient of Model Efficiency, E, was used to evaluate the performance of the hydrologic model during calibration. E ranges between -∞ and 1.0 (1 included) with E = 1 being the optimal value. Values between 0.0 and 1.0 are generally viewed as accepted levels of performance while values ≤ 0.0 indicates that the mean observed value is a better predictor than the simulated value, which indicates unacceptable model performance.

3.3 Runoff predictions in three land-cover conditions

The calibrated hydrologic model was then used to simulate surface runoff in the 11 sub-watersheds under three land-cover conditions namely, 2001, 1976 and a "rehabilitated" condition. The latter was derived from the analysis of the 2001 image, where areas in urgent need of rehabilitation were identified. This includes areas classified as grassland and barren. In the "rehabilitated" land-cover map, grassland areas were re-classified as "forest" while barren areas were converted to "agro-forested areas" which is composed of mixed vegetation. This is in accordance to the rehabilitation strategy planned by the DENR. In using the calibrated hydrologic model for predicting the impacts of land-cover change, as emphasized by the use of the three land-cover condition scenarios, only the *CN* parameter of the model that has a direct relationship with land-cover was altered. The same rainfall events used previously for model calibration were utilized again in the simulations. The results of the simulations were then analyzed (1) to determine the runoff responses of the watershed in 3 land-cover conditions, (2) to identify how different are these responses from each other, and (3) to verify if rehabilitation strategies could help in the reduction of runoff in the watershed under the assumption that the same rainfall events will take place.

4. RESULTS AND DISCUSSION

4.1 Land-cover change in the Taguibo Watershed

The land-cover maps of the study area for 1976 and 2001 derived from Maximum Likelihood-classified Landsat images are shown in Figure 3 (a and b). The 1976 land-cover map has an overall classification accuracy of 96.06% and kappa statistic of 0.95 while the 2001 land-cover map obtained 96.79% accuracy and kappa statistic of 0.96. Producer's and User's Accuracy for each land-cover type are listed in Table 4. It can be observed that the two land-cover maps are above satisfactory because of more than 90% Producer's and User's Accuracy for each land-cover class.

Comparing the two maps, we were able to determine changes in land-cover from 1976-2001 with respect to the total area of the

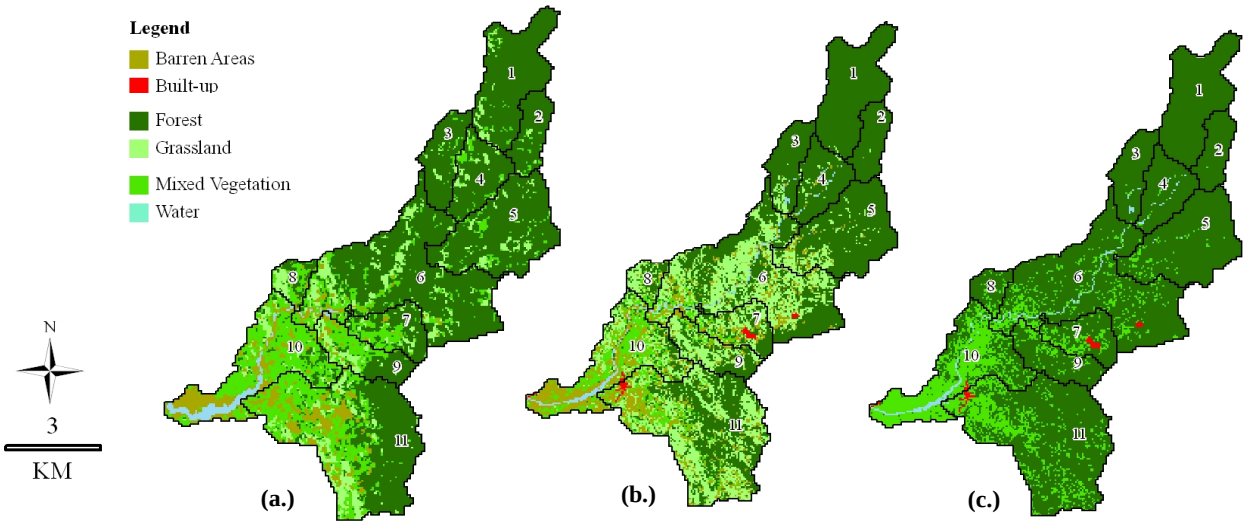

Figure 3. Land-cover maps of the Taguibo Watershed derived from the analysis of Landsat images: *(a.) 1976, (b.) 2001 and (c.) rehabilitated*. Numbers indicate sub-watersheds.

watershed (Table 5). Interestingly, the analysis showed a 6.52% reduction in forest cover, a 13.69% reduction in mixed vegetation, a 4.46% increase in barren areas and 15.54% increase in grassland in the study area in the span of 25 years. The 4.46% increase in barren areas maybe attributed to more recent human-induced alterations of the watershed such as increase in agricultural areas, forest denudation due to illegal logging and slash-and-burn farming and harvesting of planted trees (DENR, 2003). A portion of the 6.52% reduction in forest cover maybe also due to these mentioned activities. On the other hand, the reduction in mixed vegetation cover and increased in grassland areas may be the result of the historical modification of the watershed landscape by logging industries and the influx of farmers who were intent to cultivate the logged-over areas by planting high-valued vegetables and rice crops. When the potential for agricultural productivity of these areas have lessened through time, these were left over for grasses to grow (DENR, 2003). A very good basis of this is the 15.54% increase in grassland areas. As shown in the next sections, these changes in the watershed's land-cover definitely will have an effect on its hydrologic functions, especially on its runoff response to rainfall events.

Land-cover classes	1976 Land-cover Map		2001 Land-cover Map	
	PA	UA	PA	UA
Barren areas	92.50	94.87	98.15	92.98
Built-up areas	100.00	92.75	100.00	100.00
Forest	98.39	98.39	98.96	95.00
Grassland	93.10	98.18	94.51	100.00
Mixed Vegetation	93.33	96.55	100.00	100.00
Water	92.50	94.87	91.67	100.00

Table 4. Producer's (PA) and User's Accuracy (UA) of the land-cover maps (in %).

Land-cover classes	1976 Area (km^2)	2001 Area (km^2)	% Change from 1976 with respect to total watershed area
Barren areas	5.201	8.569	+4.46
Built-up areas	-	0.300	+0.40
Forest	46.287	41.366	-6.52
Grassland	7.271	19.008	+15.54
Mixed Vegetation	15.703	5.359	-13.69
Water	1.070	0.930	-0.19

Table 5. 1976-2001 land-cover change statistics.

4.2 Hydrologic model predictions of runoff

Figure 6 shows the results of the calibration of the hydrologic model with field measured data for the June 25-27, 2007 period. The computed *E* value is 0.92 indicating a highly acceptable performance. However, there are portions of the simulated hydrograph that overestimate the outflow and underestimate the peak discharge. The average residual was computed as 2.95 m^3/s. Plausible explanations for these slight differences in the simulated and measured hydrographs are the fact that the land-cover information used to parameterise during model calibration may be different to the actual land-cover of the study area when the field data were collected. Nevertheless, as the computed *E* value is very close to 1, the model could be used with modest efficiency for runoff predictions under different land-cover conditions of the watershed.

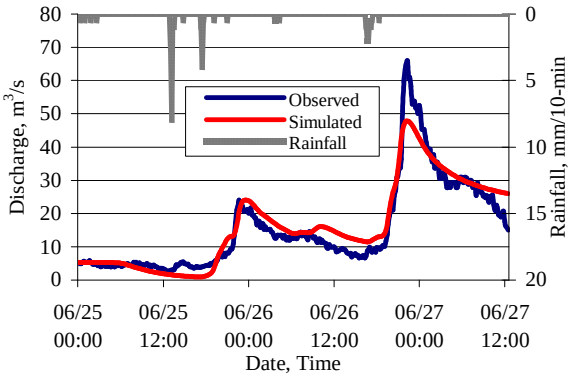

Figure 6. Hydrologic model calibration result.

4.3 Runoff predictions in 3 land-cover conditions

Figure 3c shows the "rehabilitated" land-cover map of the watershed. In this map, the watershed is in an ideal condition where barren areas and grasslands detected from the 2001

Landsat ETM+ image as consequences of anthropogenic disturbances, were rehabilitated through their conversion to mixed vegetation and reforestation, respectively.

Model predicted accumulated runoff volume at each outlet of the 11 sub-watersheds is shown in Figure 7. It can be observed that there were minimal differences in the accumulated runoff volumes in sub-watersheds 1, 2, 3 and 4 for the three land-cover conditions. This means that these sub-watersheds experienced minimal changes in land-cover. The graph also illustrated the high runoff potential of these particular sub-watersheds. Although the majority of land-cover in these areas is forest, the runoff generated during rainfall events is high. This demonstrates the effects of steep slopes and the shallowness of the soil in these areas that give minimal span for the rainwater to infiltrate the ground.

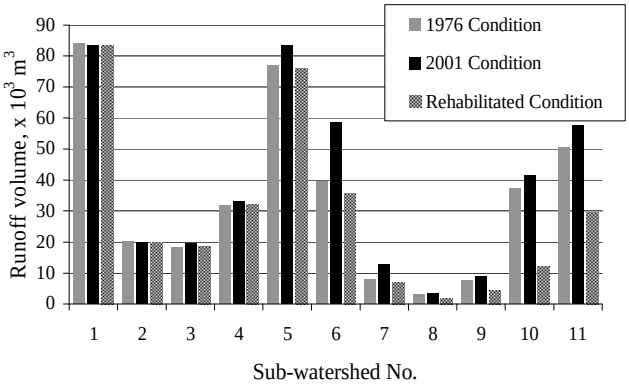

Figure 7. Model predicted accumulated runoff volume for the 11 sub-watersheds from June 25-27, 2007 under 3 land-cover conditions.

Pronounced variation in runoff volumes were observed for the remaining watersheds in the 1976 and 2001 land-cover conditions, most especially in sub-watersheds 5, 6, 7, 9, 10 and 11. It can be stated that changes in major land-cover types in these areas, specifically the increase of barren areas and grasslands and the decrease in forest and mixed vegetation covers (Table 8) have directly affected the hydrologic response of the watershed to rainfall events – rainfall interception and infiltration have been affected such that huge volumes of surface runoff are generated. In terms of total surface runoff accumulated at the main outlet of the watershed (Table 9), model predictions showed that accumulated runoff volume in 1976 were 10.62% lesser than in 2001. Rehabilitation of the sub-watersheds through planting of mixed vegetation and reforestation was found effective. We computed that it reduced the accumulated runoff volume in 2001 by 23.85%. These results provide quantitative estimations that rehabilitation strategies proposed by the DENR, should they be 100% implemented, are most likely to reduce the volume of runoff generated during rainfall events in the Taguibo Watershed.

SW No.	Area, km^2	% change in Barren Areas	% change in Forest	% change in Grassland	% change in Mixed Vegetation
5	8.748	+3.80	-3.68	+5.91	-6.20
6	16.483	+7.27	-26.95	+27.05	-8.96
7	3.224	+12.52	-18.22	+25.93	-23.51
9	3.459	+2.71	+1.91	+24.05	-27.82
10	9.056	+9.01	+3.35%	+13.64	-21.12
11	16.540	+2.39	-5.66%	+23.84	-21.20

Table 8. Major land-cover change from 1976-2001 in sub-watersheds (SW) 5, 6, 7, 9, 10 and 11. Percentage of change is computed with respect to the area of the sub-watershed.

The results of the hydrologic model simulations indicate that significant increase in runoff volumes during rainfall events can be attributed to the reduction in forest and mixed vegetation cover due to their conversions to grasslands and barren areas. These results are consistent with those of Costa et al. (2003) and Siriwaderna et al. (2006).

Land-cover condition	Accumulated watershed runoff volume, $x10^3$ m^3	% Difference from the 2001 condition
1976	376.771	- 10.62%
2001	421.540	
Rehabilitated	320.996	-23.85%

Table 9. Accumulated runoff volumes in 3 land-cover conditions (total for 11 sub-watersheds) for the June 25-27, 2007 period.

5. CONCLUSIONS

We have presented an analysis of 25-year land-cover change in the critical Taguibo Watershed in Mindanao, Philippines using post-classification comparison analysis of Maximum Likelihood-classified Landsat images. We expanded our analysis by incorporating the detected changes in land-cover to a GIS-based hydrologic model. This allowed us to better understand the impacts of the land-cover change to the increase in surface runoff during rainfall events in the Taguibo Watershed. The Landsat image analysis also provided us a very quick identification of areas that need rehabilitation. Using the hydrologic model, we tested planned rehabilitation strategies that were aimed to reduce surface runoff, and we were able to express the effectiveness of these strategies. One of the most important results of this study is that we were able to establish the direct relationship between forest and mixed vegetation cover reduction to increases in surface runoff.

In conclusion, this study has demonstrated the usefulness of multi-temporal Landsat images in detecting land-cover change, in identifying areas for rehabilitation, and in evaluating rehabilitation strategies for management of tropical watersheds through its use in hydrologic modeling. Although the methods used in this study was applied in a relatively small watershed, its applicability to large watersheds and river basins is also possible as long as there are available Landsat images to derive land-cover information needed for detecting and locating the changes, and for hydrologic modeling. With the availability over the internet of Landsat images acquired since 1972, the methods employed in this study can be readily applied for watershed land-cover change monitoring, management and rehabilitation. Moreover, this study made use of the MLC in Landsat image classification. While the land-cover maps derived from the classifications are highly accurate, it is mainly due to the satisfaction of the assumptions of the MLC for class signatures to be normally distributed, and to the high degree of separability of the class signatures. In some cases, the number of training samples to obtain class signatures is limited and/or may not have normal distributions, which restricts the MLC to get the ideal result. The use of other classifiers such as DT, NN and SVM can solve this problem but at the cost of increase in computation time.

REFERENCES

Bach, H., Braun, M., and Mauser, W., 2003. Use of remote sensing for hydrological catchments. *Hydrology and Earth System Sciences*, 7(6), pp. 862-876.

Bhuyan, S.J., Koelliker, J.K., Marzen, L.J., and Harrington Jr., J.A., 2003. An integrated approach for water quality assessment of a Kansas watershed. *Environmental Modelling & Software*, 18, pp. 473-484.

Cebecauer, T. and Hofierka, J., 2008. The consequences of land-cover changes on soil erosion distribution in Slovakia. *Geomorphology*, 98(3-4), pp. 187-198.

Cherrill, A.J., Lane, A., and Fuller, R.M., 1994. The use of classified Landsat 5 Thematic Mapper imagery in the characterization of landscape composition: a case study in Northern England. *Journal of Environmental Management*, 40(4), pp. 357-377.

Chow, V.T., Maidment, D.R., and Mays, L.W., 1988. *Applied Hydrology*. McGraw-Hill: New York, USA.

Chowdhury, R., 2006. Landscape change in the Calakmul Biosphere Reserve, Mexico: Modeling the driving forces of smallholder deforestation in land parcels. *Applied Geography*, 26(2), pp. 129–152.

Cingolani, A.M., Renison, D., Zak, M.R., and Cabido, M.R., 2004. Mapping vegetation in a heterogeneous mountain rangeland using Landsat data: an alternative method to define and classify land-cover units. *Remote Sensing of Environment*, 92(1), pp. 84-97.

Coppin, P., I. Jonckheere, K. Nackaerts, and Muys, B., 2004. Digital change detection methods in ecosystem monitoring: a review. *International Journal of Remote Sensing*, 25, no. 9, pp. 1565–1596.

Costa, M.H., Botta, A., and Cardille, J.A., 2003. Effects of large-scale changes in land cover on the discharge of the Tocantins River, Southeastern Amazonia. *Journal of Hydrology*, 283(1-4), pp. 206-217.

DENR, 2003. *Taguibo River Watershed Management Plan*. Department of Environment and Natural Resources, Caraga Region XIII, Butuan City, Agusan del Norte, Philippines.

Engman, E.T., 1995. The use of remote sensing data in watershed research. *Journal of Soil and Water Conservation*, 50(5), pp. 438-440.

Engman, E.T., 1996. Remote sensing applications to hydrology: future impact. *Hydrological Sciences*, 41(4), pp. 637-647.

Hagner, O., and Reese, H., 2007. A method for calibrated maximum likelihood classification of forest types. *Remote Sensing of Environment*, 110(4), pp. 438-444.

Helmschrot, J. and Flügel, W.A., 2002. Land use characterization and change detection analysis for hydrological model parameterization of large scale afforested areas using remote sensing. *Physics and Chemistry of the Earth*, 27(9-10), pp. 711-718.

Huang, C., Davis, L.S., and Townshend, J.R.G., 2002. An assessment of support vector machines for land cover classification. *International Journal of Remote Sensing*, 23(4), pp. 725–749.

Jensen, J.R., 2004. *Introductory Digital Image Processing: A Remote Sensing Perspective*. New Jersey: Prentice-Hall.

Leblanc, M.J., Favreau, G., Massuel, S., Tweed, S.O., Loireau, M., and Cappelaere, B., 2008. Land clearance and hydrological change in the Sahel: SW Niger. *Global and Planetary Change*, 61(3-4), pp. 135-150.

McColl, C. and Aggett, G., 2007. Land-use forecasting and hydrologic model integration for improved land-use decision support. *Journal of Environment Management*, 84(4), pp. 494-512.

Melesse, A.M., and Shih, S.F., 2002. Spatially distributed storm runoff depth estimation using Landsat images and GIS. *Computers and Electronics in Agriculture*, 37, pp. 173-183.

Muttitanon, W., and Tripathi, N.K., 2005. Land use/land cover changes in the coastal zone of Ban Don Bay, Thailand using Landsat 5 TM data. International Journal of Remote Sensing, 26(11), pp. 2311–2323.

Nash, J., and Sutcliffe, J., 1970. River flow forecasting through conceptual models, I - A discussion of principles. *Journal of Hydrology*, 10, pp. 282-290.

O'Connell, E., Ewen, J., O'Donnell, G., and Quinn, P., 2007. Is there a link between agriculture land-use management and flooding? *Hydrology & Earth System Sciences*, 11(1), pp. 96-107.

Otukei, J., and Blaschke, T., 2010. Land cover change assessment using decision trees, support vector machines and maximum likelihood classification algorithms. *International Journal of Applied Earth Observation and Geoinformation*, 12(Supplement 1), S27-S31.

Pandey, A., Chowdary V.M., Mal, B.C., and Billib M., 2008. Runoff and sediment yield modelling from a small agricultural watershed in India using the WEPP model. *Journal of Hydrology*, 348 (3-4), pp. 305-319.

Ponce, V.M., Hawkins, R.H., 1996. Runoff curve number: has it reached maturity? *Journal of Hydrologic Engineering*, 1, pp. 11-19.

Richards, J.A., and Jia, X., 1997. *Remote Sensing Digital Image Analysis, An Introduction*, Third Edition, Springer-Verlag.

Schowengerdt, R.A., 1997. *Remote Sensing: Models and Methods for Image Processing*, Second Edition, Academic Press.

SCS, 1985. *National Engineering Handbook, Section 4: Hydrology*. Soil Conservation Service, US Department of Agriculture, Washington D.C.

Shuying, J., Deren, L., and Jingwen, W., 2005. A comparison of support vector machine with maximum likelihood classification algorithms on texture features. *Proceedings of IEEE*

International Geoscience and Remote Sensing Symposium, pp. 3717-3720.

Siriwaderna, L., Finlayson, B.L., McMahon, T.A., 2006. The impact of land use change on catchment hydrology in large catchments: The Comet River, Central Queensland, Australia. *Journal of Hydrology*, 326, pp. 199-214.

Swain, P.H. & Davis, S.M., 1978. *Remote sensing: the quantitative approach*, McGraw-Hill New York.

USACE, 2000. *Hydrologic Modeling System HEC-HMS Technical Reference Manual*. United States Army Corps of Engineers-Hydrologic Engineering Center: Davis, California.

USACE, 2003. *Geospatial Hydrologic Modelling Extension HEC-GeoHMS User's Manual, Version 1.1*. United States Army Corps of Engineers-Hydrologic Engineering Center: Davis, California.

Vafeidis, A.T., Drake, N.A., and Wainwright, J., 2007. A proposed method for modeling the hydrologic response of catchments to burning with the use of remote sensing and GIS. *Catena*, 70(3), pp. 396-409.

Vagen, T.G., 2006. Remote sensing of complex land use change trajectories—a case study from the highlands of Madagascar. *Agriculture, Ecosystems and Environment*, 115(1-4), pp. 219–228.

Van Genderen, J.L., Lock, B.F., and Vass, P.A., 1978. Remote sensing: statistical testing of thematic map accuracy. *Remote Sensing of Environment*, 7, pp. 3-14.

ACKNOWLEDGEMENTS

Funding for this research was provided by the Philippine Council for Advanced Science and Technology Research and Development of the Department of Science and Technology (PCASTRD-DOST) through a local graduate scholarship grant to the first author. Engrs. Alexander S. Caparas, Jessie Linn P. Ablao (of UP Diliman) and Michelle V. Japitana (CSU) assisted us during the field surveys. The Field Operations Center of the Philippine Atmospheric Geophysical and Astronomical Services Administration (PAGASA) provided the tipping bucket rain gauge used in this study. The authors would like to thank two anonymous reviewers for their helpful comments and suggestions.